

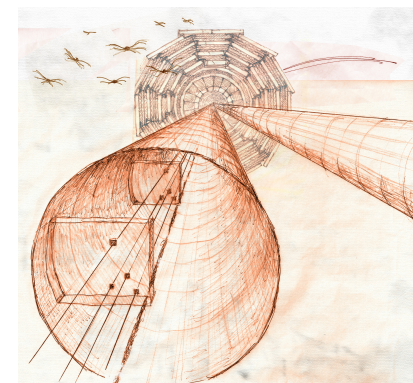
The Precision Proton Spectrometer of CMS: performance and upgrade

A. Solano on behalf of the CMS and TOTEM Collaborations

Università di Torino and INFN



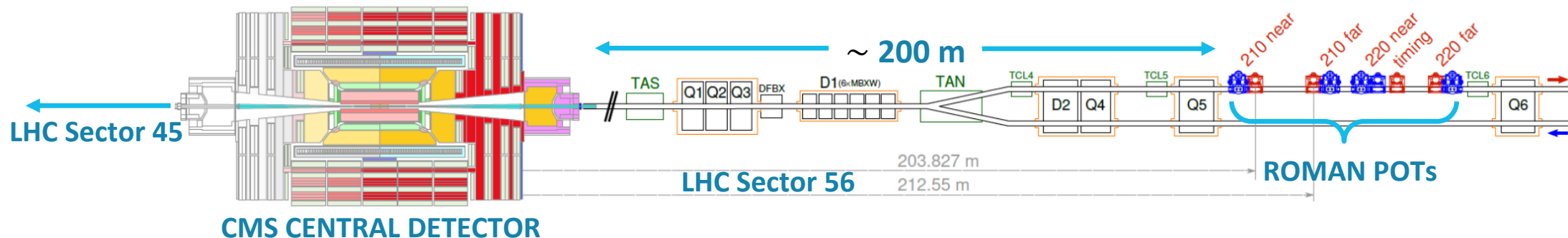
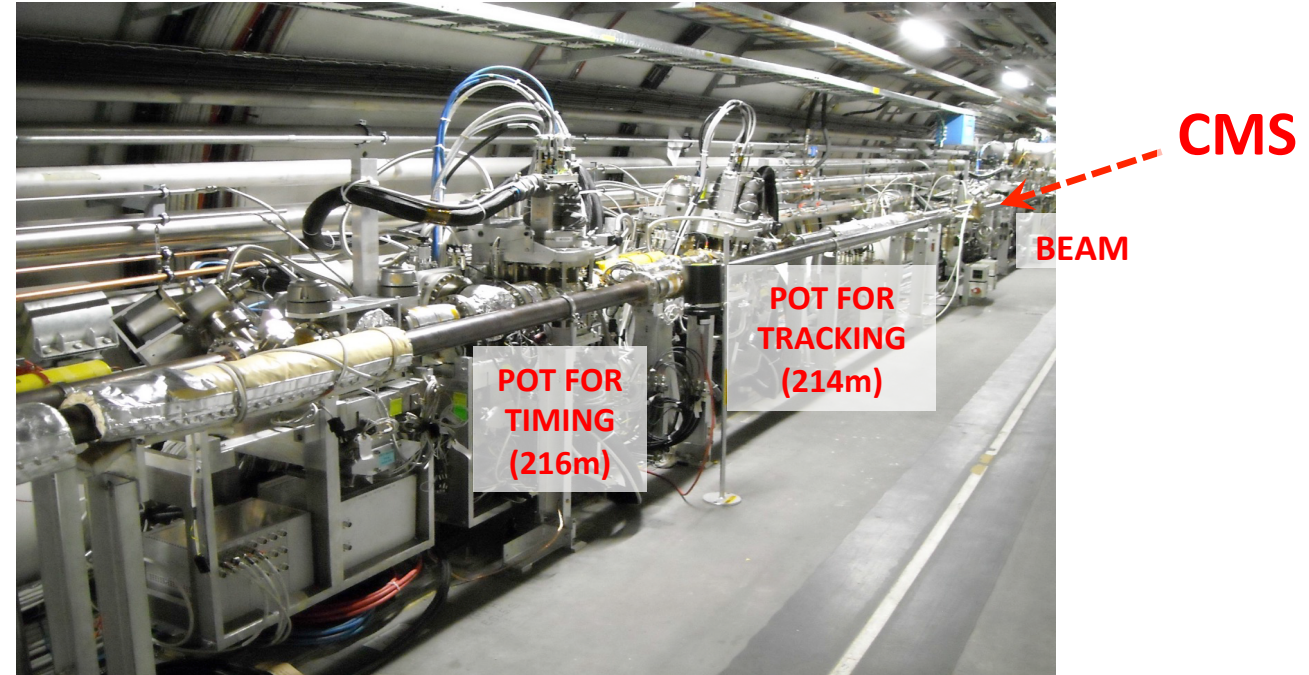
ICHEP 2020
30/7/2020



Outline

- Project overview
- Experimental apparatus
- Detector performance in LHC-Run2
- Upgrades for LHC-Run3

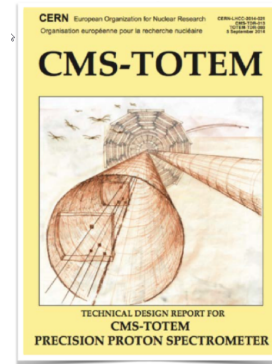
Roman pots along the LHC tunnel



The CT-PPS - now PPS - project

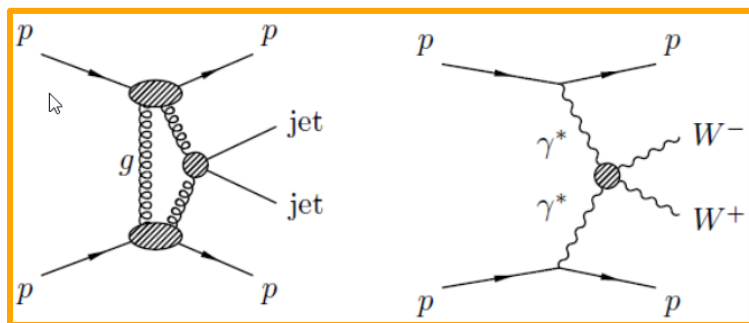
The CMS-TOTEM Precision Proton Spectrometer (CT-PPS) has been **designed for measuring the scattered protons** on both sides of CMS in **standard LHC running conditions**, using LHC magnets to measure the proton momentum [TDR CERN-LHCC-2014-021].

Since April 2018, CT-PPS is a standard component of CMS, with name PPS.

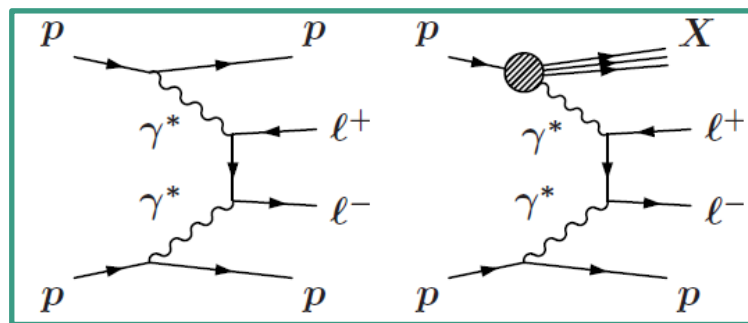


The PPS physics program focuses on **Central Exclusive Production (CEP)** processes of the type:

$pp \rightarrow pXp$ with $X = \text{high-}E_T \text{ jets, } WW, ZZ, \gamma\gamma, \dots$



Processes studied in detail for the TDR



PPS first publication, JHEP07 (2018) 153

$$M_{pp} = M_X = \sqrt{s\xi_1\xi_2}$$

- **Tracking detectors** measure the proton displacement w.r.t. the beam, which is translated into the proton fractional momentum loss (ξ) thanks to the knowledge of the beam optics
- **Timing detectors** are used to disentangle pileup
- All are located inside Roman Pots so that they can be moved very close to the circulating beams

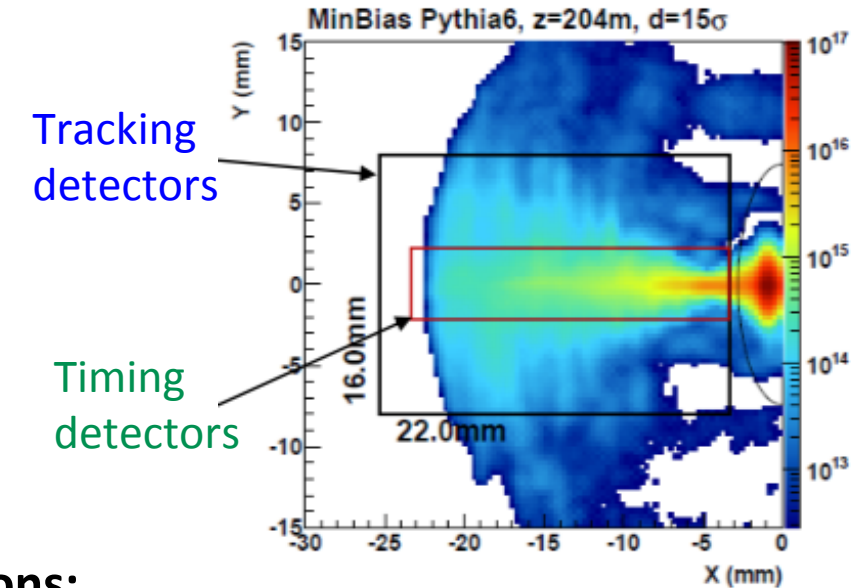
Experimental challenge and apparatus in LHC-Run2

- Roman Pots need to operate at few mm from the beam (~ 1.5 mm) to maximize acceptance

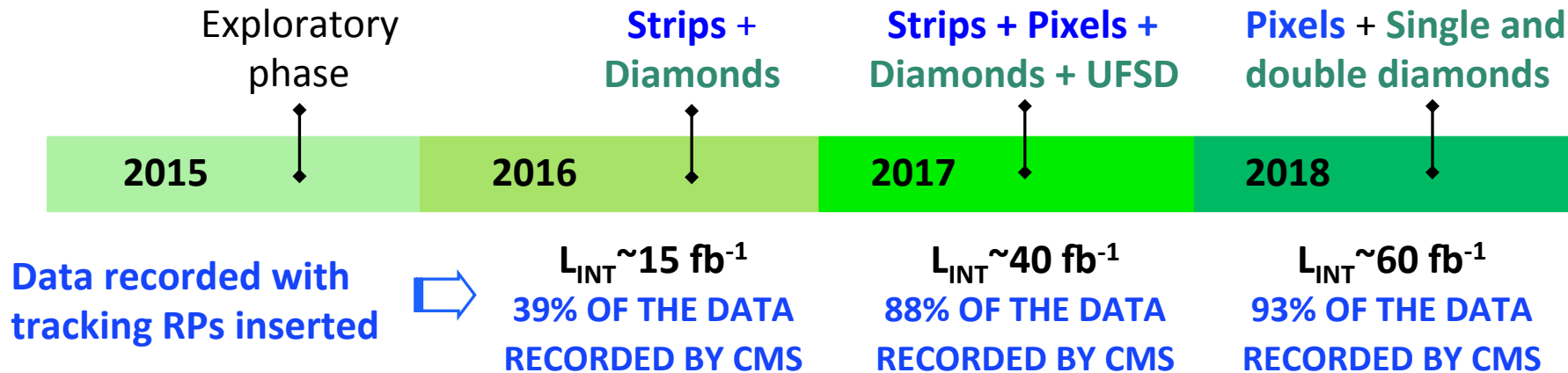
-> Detectors must tolerate high levels of non-uniform irradiation

- Proton fluence up to $\sim 5 \times 10^{15}$ protons/cm² for 100 fb⁻¹ (Run2)
Dose: ~ 1.61 Mrad/fb⁻¹

- **Spatial resolution goal:** ~ 10 -30 μ m
- **Timing resolution goal:** ~ 20 -30 ps



Data taking in 2016, 2017 and 2018 with different detector configurations:



Very high stability in both 2017 and 2018

PPS integrated luminosity in Run2:
 ~ 115 fb⁻¹

Detectors

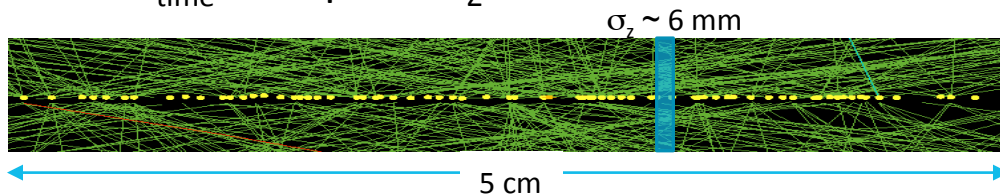
Tracking detectors

- Aim: measure proton momentum
 - ▷ Detailed knowledge of the LHC optics required
- Technologies:
 - ▷ **Silicon Strips**
 - ▷ **3D Silicon Pixels** (radiation hard, high granularity and 'edgeless')

Timing detectors

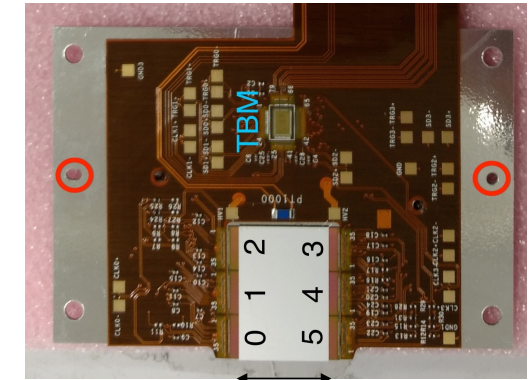
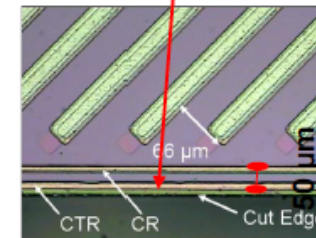
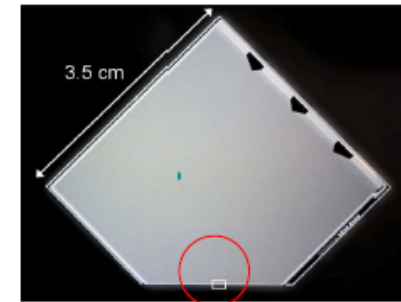
- Aim: disentangle primary vertex from pileup

$$\sigma_{\text{time}} \sim 30 \text{ ps} \rightarrow \sigma_z \sim 6 \text{ mm}$$

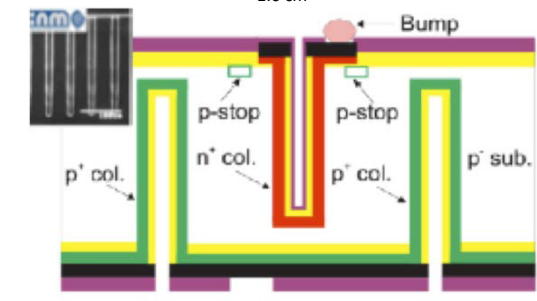


- Technologies:
 - ▷ **Single-diamonds (SD)** and **Double-diamonds (DD)**
 - ▷ **Ultra-Fast Silicon Detectors (UFSD)**

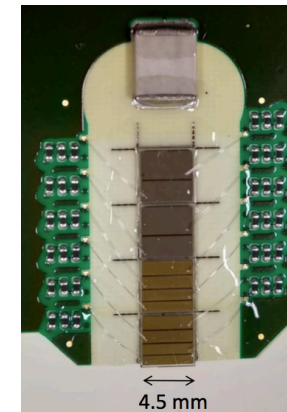
Strips



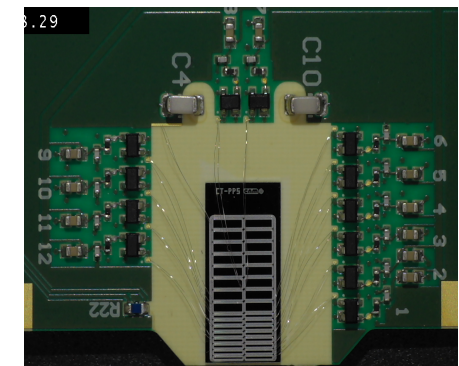
3D pixels



Diamonds



UFSD



2D impact point distributions on tracking detectors

LHC SECTOR 45

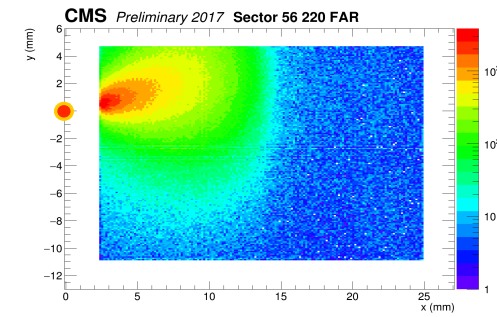
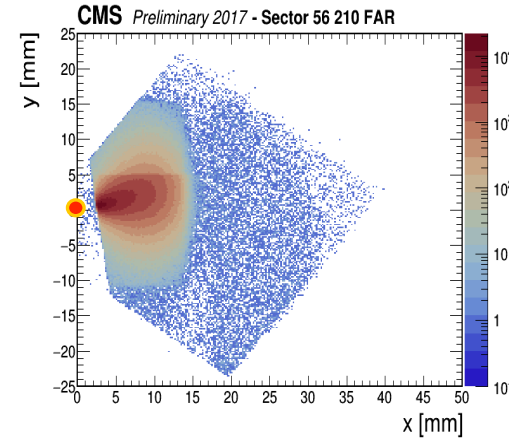
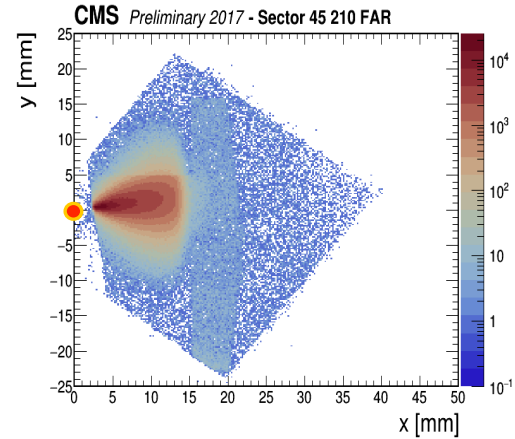
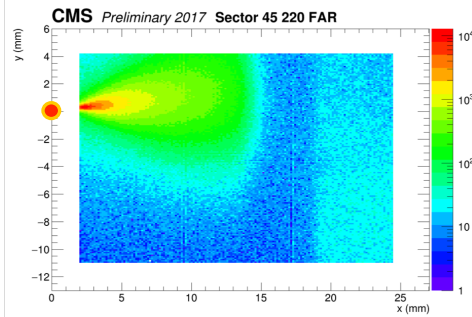
IP5

LHC SECTOR 56

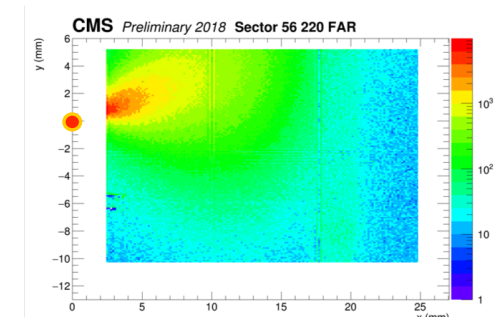
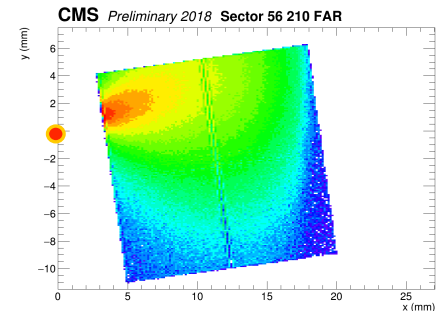
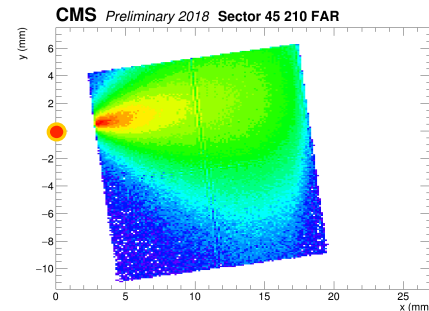
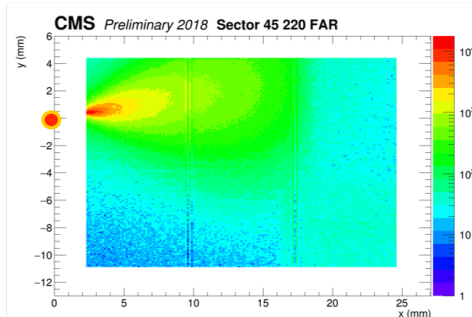
● BEAM

[always in $x=0, y=0$]

2017 DETECTOR CONFIGURATION



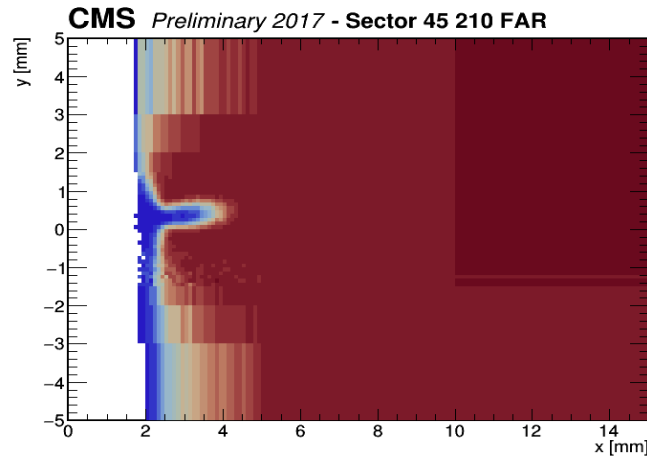
2018 DETECTOR CONFIGURATION



The RPs located at 210 m are tilted by 8° around the z axis.

Si-strip detector efficiency (2017)

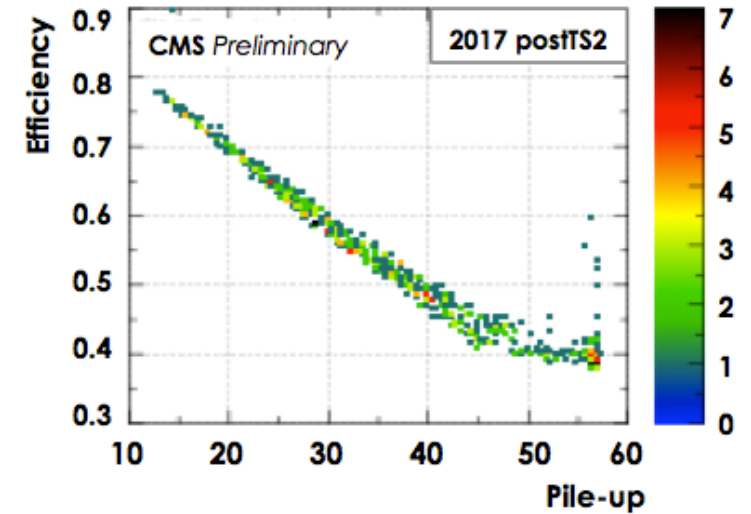
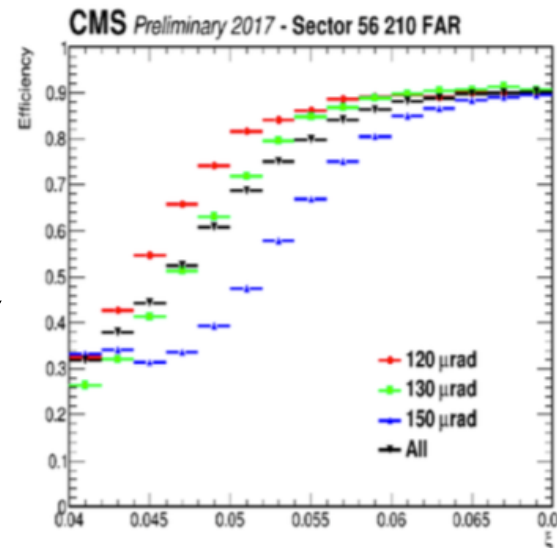
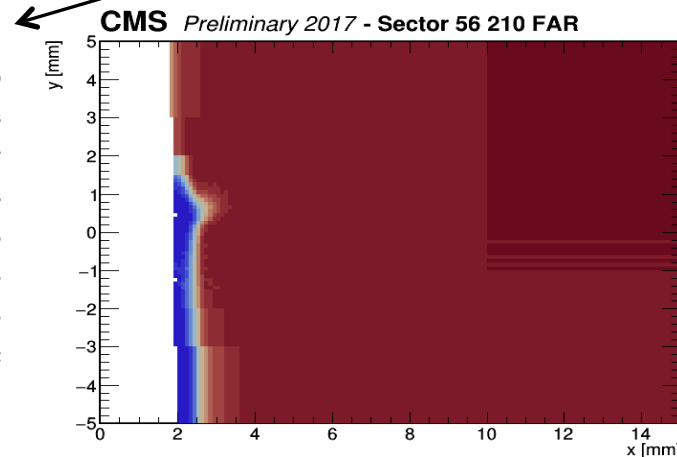
Two major sources of inefficiency (**radiation damage** and **no multi-track capability**) studied separately



$\sim 9 \text{ fb}^{-1}$

Radiation damage in the area close to the beam is clearly visible

Efficiencies as a function of ξ are computed separately for each of the main LHC crossing angles used in 2017

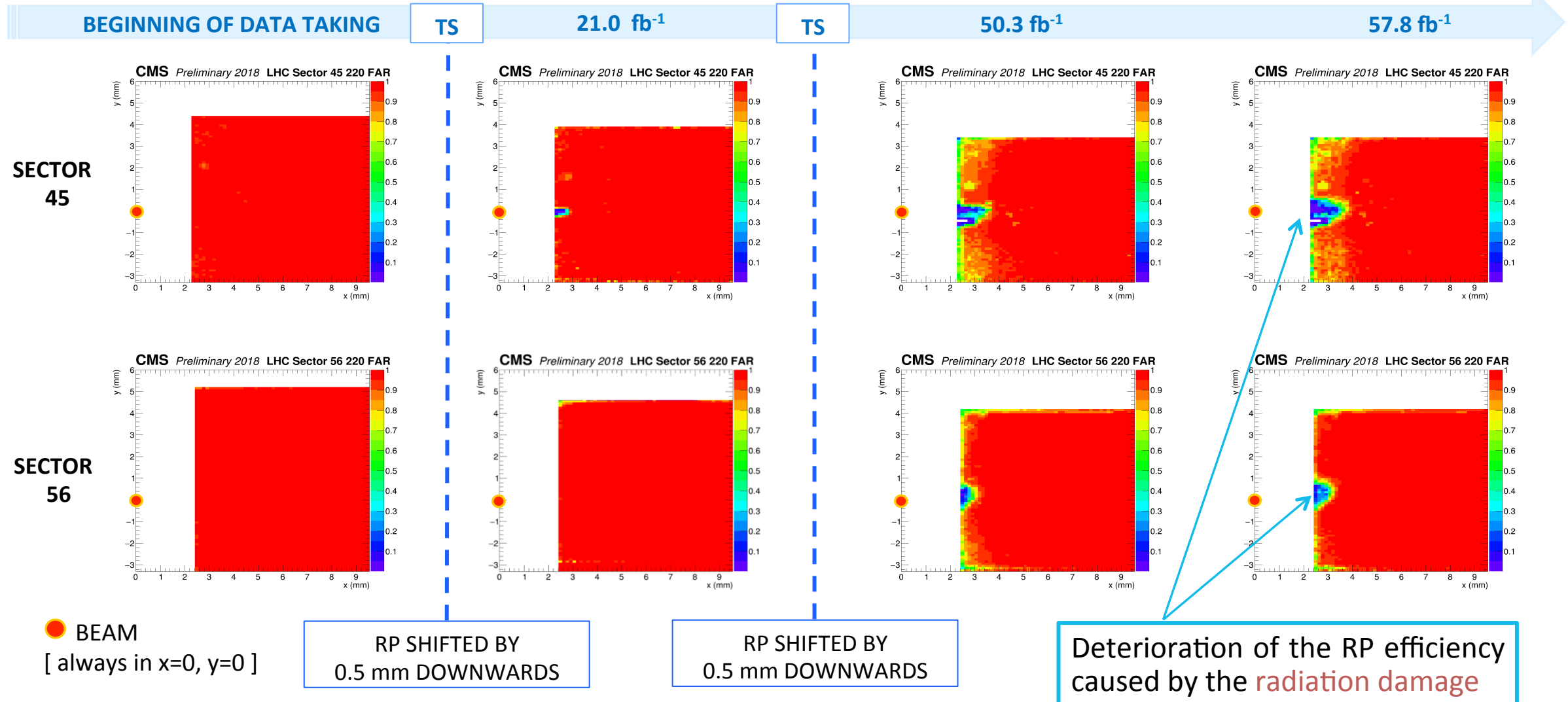


Only single-track events can be reconstructed with the strip detector

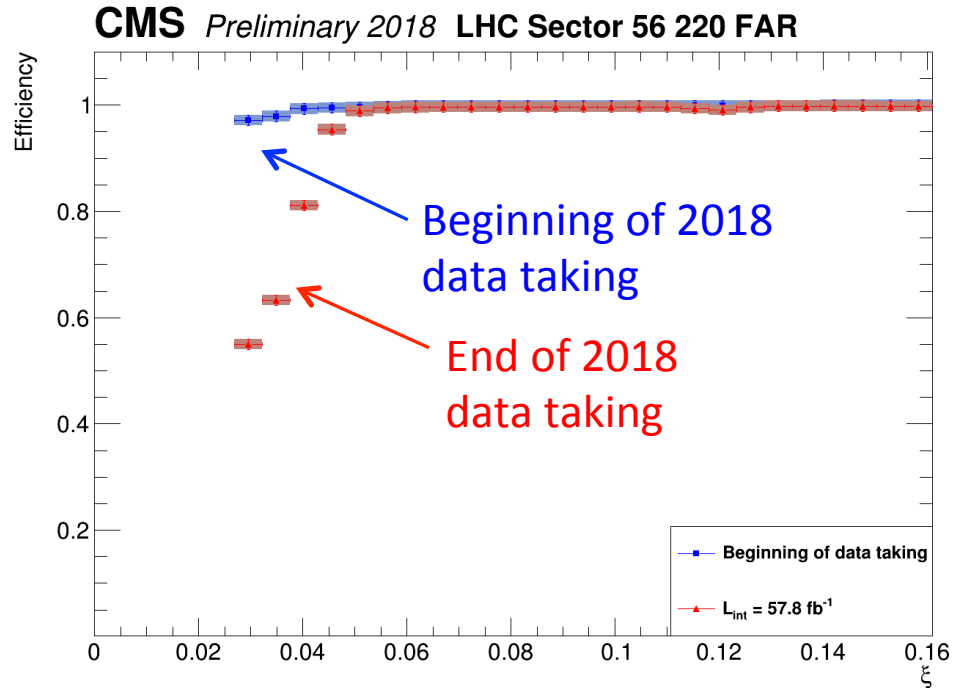
The increasing number of multi-track events with pileup shows the advantage of a pixel detector w.r.t. a strip one

3D pixel detector efficiency (2018)

Evolution of the RP efficiency maps in the detector region closest to the beam for RP 220 FAR (worst case)

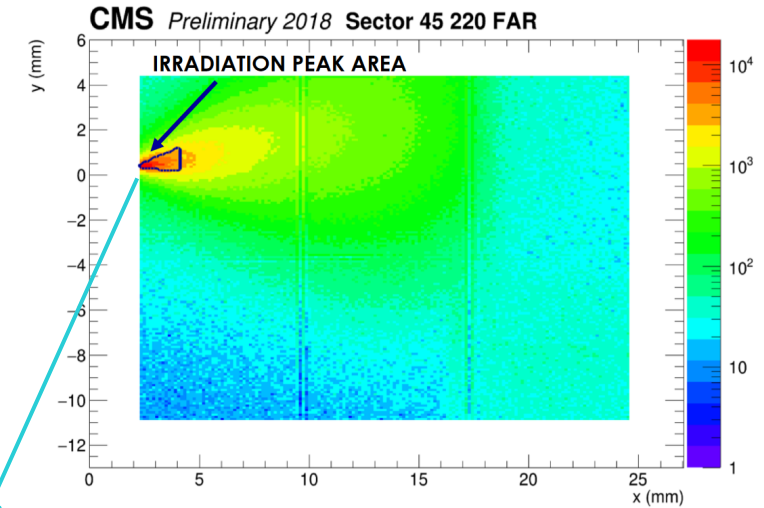


3D pixel detector efficiency (2018)



The **radiation damage** in the highest irradiated region affects the detector performance at low ξ

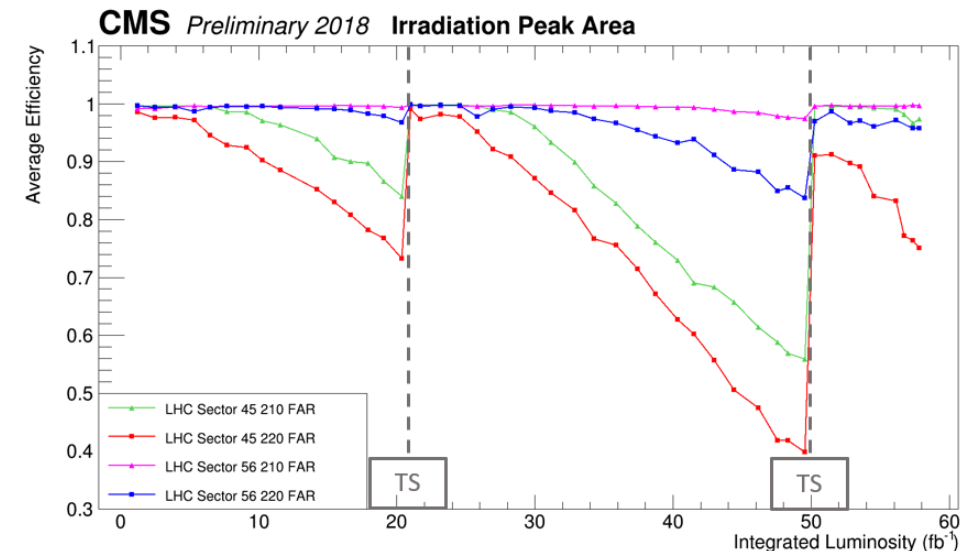
-> Impact on physics analyses



Average efficiency calculated every 1 fb^{-1} in the critical region (irradiation peak area):

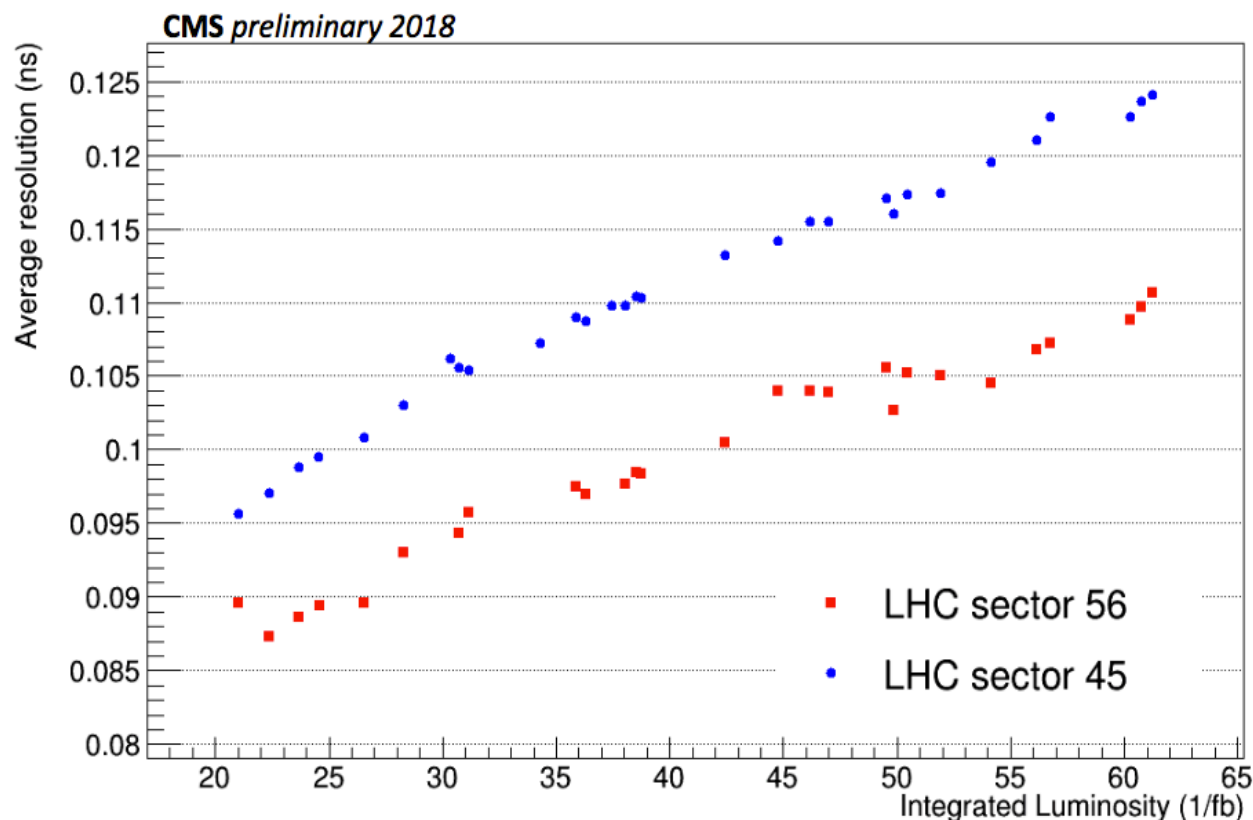
- **Recovery after each Technical Stop (TS)** because of the vertical movement of the RPs

Outside the irradiation peak area the efficiency remains high (>95%) and constant during all data taking



Proton timing resolution (2018)

This is a measurement of the full timing station resolution (sensor + front-end + digitization + timing channel calibration and reconstruction procedure)



1 track in both pixel tracker stations &
4 diamond planes & 1 pad per plane

Timing detectors can be used for physics.

With 2018 performance important background reduction can be achieved.

Tracking and timing detectors for LHC-Run3

PPS will operate as a full CMS subsystem in LHC-Run3 (2022 - 2024)

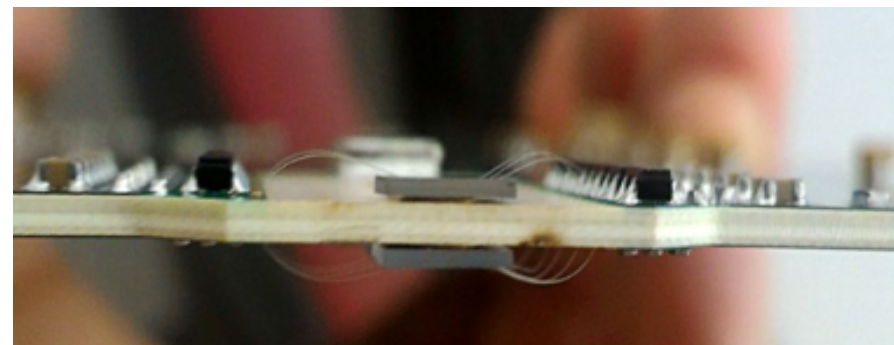
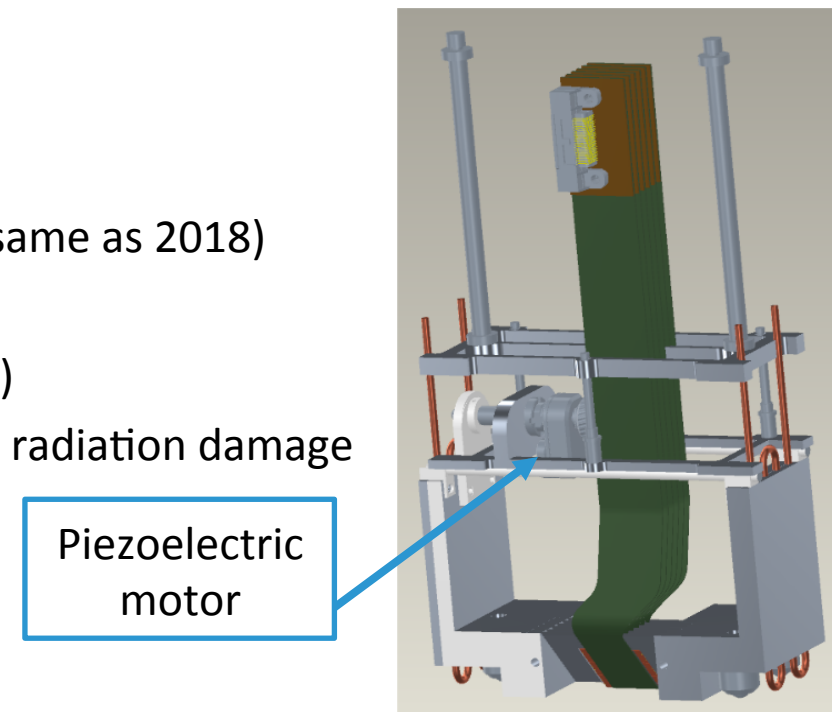
TRACKER SYSTEM in LHC-Run3

- 2 RPs per side, at 210 m and 220 m from CMS-IP with 6 detector planes per RP (same as 2018)
- New **3D silicon pixel sensors**, produced at FBK in single-side technology and bump-bonded to the **PROC600** chip (same as layer 1 of CMS central pixel tracker)
- **New detector package with internal movement system**, to better distribute the radiation damage
 - 12 positions spaced by 500 μm , possibility of handling **more than 50 fb⁻¹ with minimal efficiency loss**

TIMING SYSTEM FOR LHC-Run3

- An **important upgrade program** is ongoing, both **on electronics and sensors**
- An additional timing station will be built and installed in each sector
 - **8 DD planes in each sector**

Ultimate resolution goal (< 30 ps) within reach



Conclusions

PPS has proven the feasibility of continuously operating a near-beam proton spectrometer at a high-luminosity hadron collider and has collected $\sim 115 \text{ fb}^{-1}$ of data during LHC-Run2

- **The tracking system** has been **successfully operated** since the beginning of LHC-Run2 with very high stability and **overall very good performance**, despite the high and non-uniform irradiation
- **The timing system performance in 2018 is sufficient to reduce pileup background in CEP processes.**
Studies of the vertex resolution are ongoing

PPS will continue its program in LHC-Run3 with the goal of a total integrated luminosity of $\sim 300 \text{ fb}^{-1}$

- **New 3D silicon pixel sensors** read out by the PROC600 chip will be installed in the 4 tracking stations
- **A remotely controlled movement system** will allow to shift the tracking detector packages to mitigate the efficiency degradation due to irradiation
- **Important upgrades are ongoing for the timing system**, with the ultimate goal of a timing resolution $< 30 \text{ ps}$

Studies of a PPS detector for HL-LHC have recently converged into an EoI draft, endorsed by CMS and sent to the LHCC

Last but not least, we have a rich program of physics analyses!

At this conference, see the talk of J.A. Williams (28/7) “Searches for new physics using final states with photons”, with a search for exclusive diphotons with intact protons

Backup

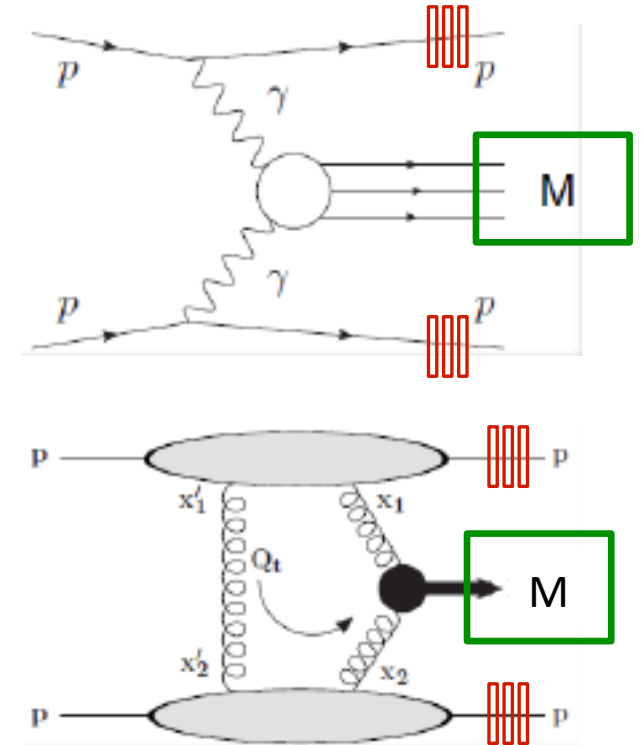
PPS physics motivation

Experimental strategy

- High- p_T system detected by the **CMS central detector** together with very low angle scattered protons detected by **PPS**
- Requiring the momentum balance between the central system and the detected protons creates **strong kinematical constraints**
- **Central system mass M can be measured via the momentum loss of the two protons**

Physics

- **EWK:** LHC as $\gamma\gamma$ collider with tagged protons
 - Measurement of $\gamma\gamma \rightarrow W^+W^-, e^+e^-, \mu^+\mu^-, \tau^+\tau^-$
 - Search for aQGC with high sensitivity
 - Search for SM forbidden $ZZ\gamma\gamma, \gamma\gamma\gamma\gamma$ couplings
- **QCD:** LHC as gg collider with tagged protons
 - Exclusive two- and three-jets event
 - Tests of pQCD mechanism of exclusive production
 - Gluon jet samples with small component of quark jet
- **BSM**
 - Clean events (no underlying pp events)
 - Independent mass measurement by pp system
 - J^{PC} quantum numbers $0^{++}, 2^{++}$



PPS experimental apparatus in 2018

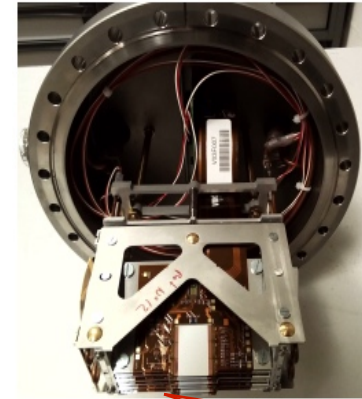
➤ PPS → High Luminosity Runs

- ▷ 2 pots with 3D Silicon Pixel for Tracking
- ▷ 1 pot with 2 Diamond + 2 Double-Diamond planes for Timing

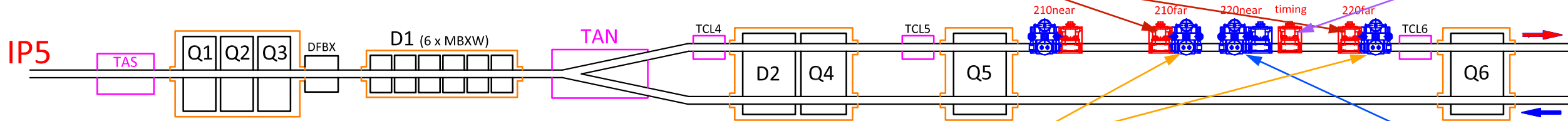
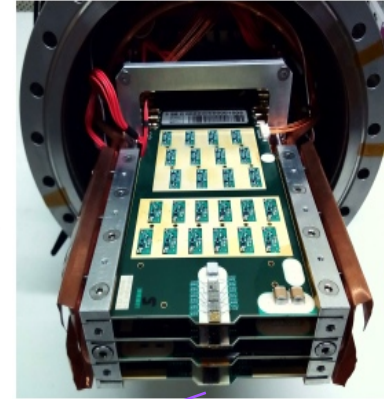
➤ CMS-TOTEM → Low Luminosity special Runs

- ▷ 2 pots with Silicon Strip planes for Tracking
- ▷ 1 pot with UFSD planes for Timing

6 planes of
3D Silicon Pixel
Detectors [H]



2 planes of
Diamond +
2 planes of
Double Diam.
Detectors [H]

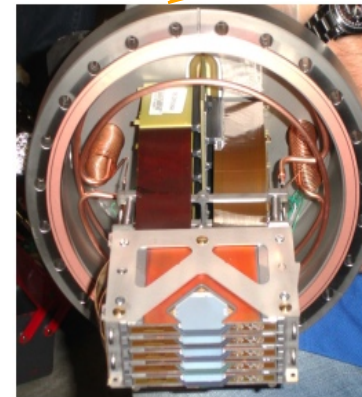


[H] PPS Horizontal Roman Pots
for high lumi - low β^* runs
(high PU)

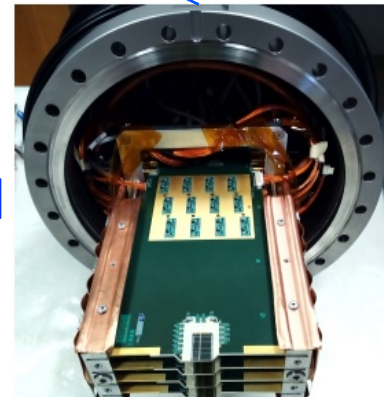
[V] CMS-TOTEM Vertical Roman Pots
for low lumi - high β^* runs
(low PU)

→ to access central exclusive production of low mass systems

10 planes of
Silicon Strip
Detectors [V]



4 planes
of UFSD [V]

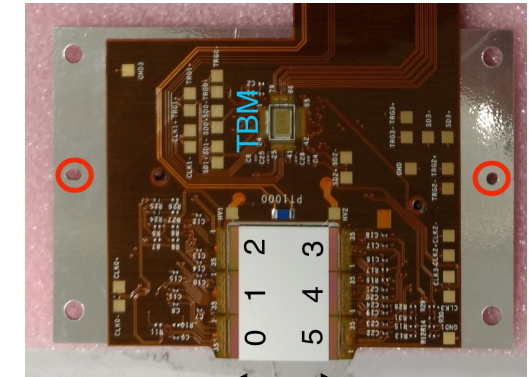
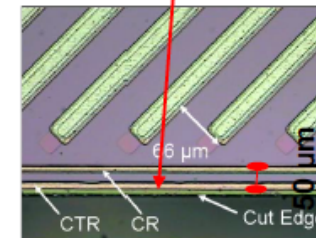


Detectors

Tracking detectors

- Aim: measure proton momentum
 - ▷ Detailed knowledge of the LHC optics required
- Technologies:
 - ▷ **Silicon Strips**
 - ▷ **3D Silicon Pixels** (radiation hard, high granularity and 'edgeless')

Strips

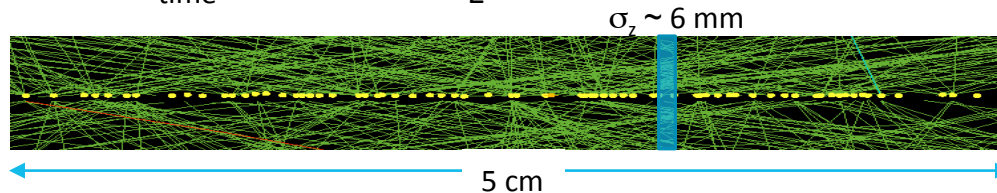


3D pixels

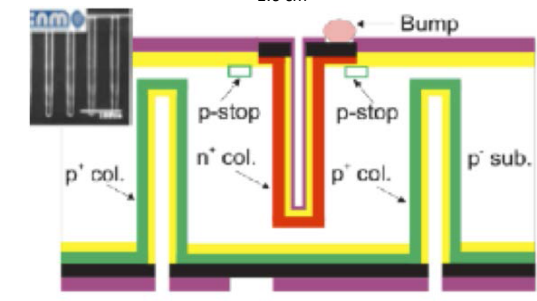
Timing detectors

- Aim: disentangle primary vertex from pileup

$$\sigma_{\text{time}} \sim 30 \text{ ps} \rightarrow \sigma_z \sim 6 \text{ mm}$$

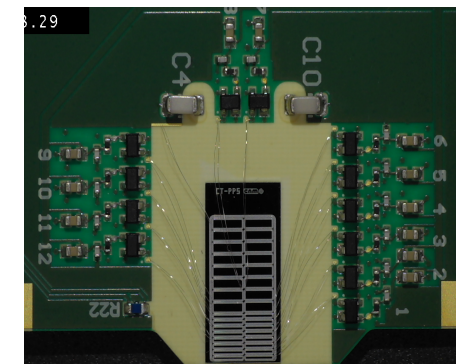
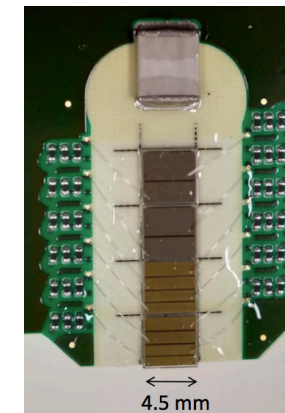


$$\sigma_{z_{\text{vtx}}} = \frac{c}{2} \sqrt{2\sigma_{\Delta t}^2} \quad \begin{matrix} \sigma_{\Delta t} = 10 \text{ ps} & \approx & 2 \text{ mm} \\ \sigma_{\Delta t} = 30 \text{ ps} & \approx & 6 \text{ mm} \end{matrix}$$



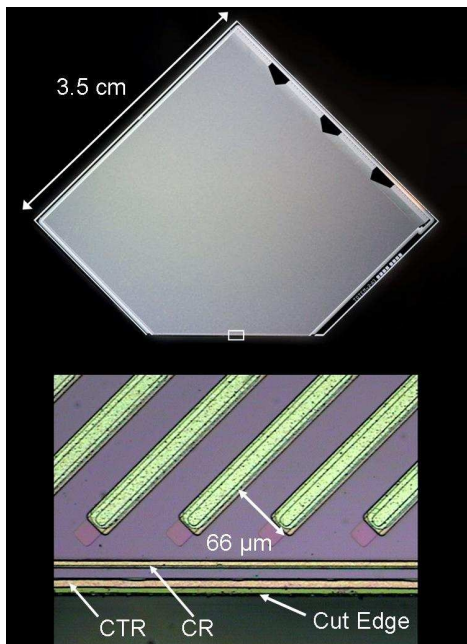
- Technologies:
 - ▷ **Single-diamonds and Double-diamonds**
 - ▷ **Ultra-Fast Silicon Detectors (UFSD)**

Diamonds



UFSD

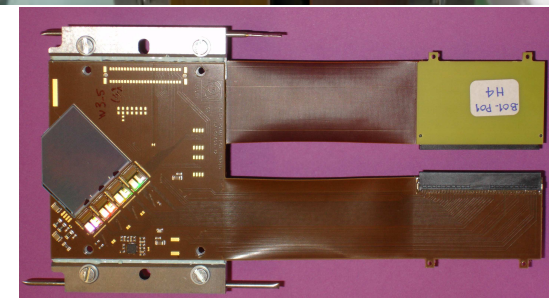
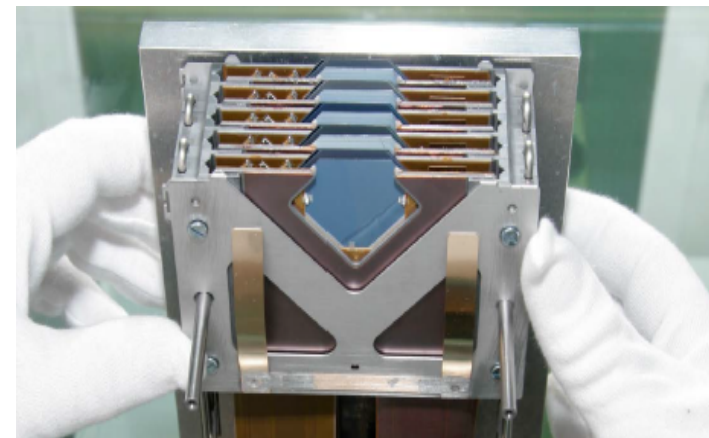
Tracking detector - Silicon strips



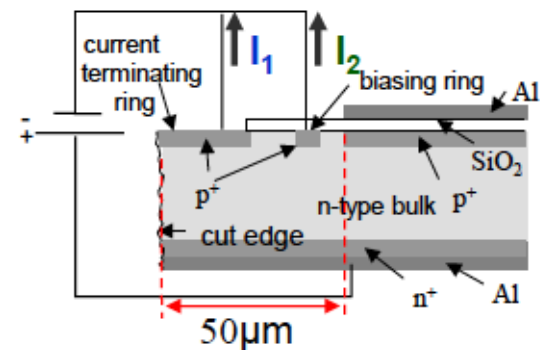
Same detectors used by the TOTEM experiment^[*]

10 planes per pot of silicon strip detectors

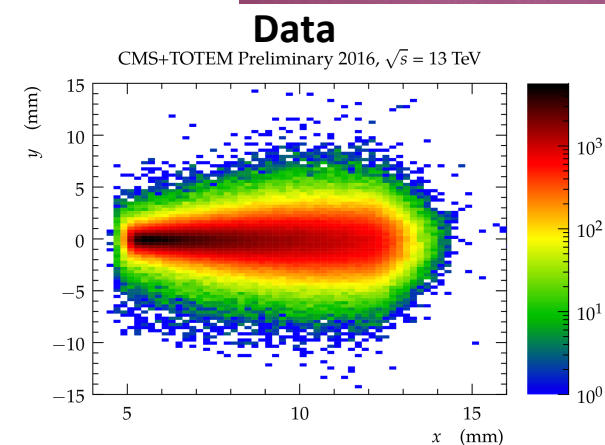
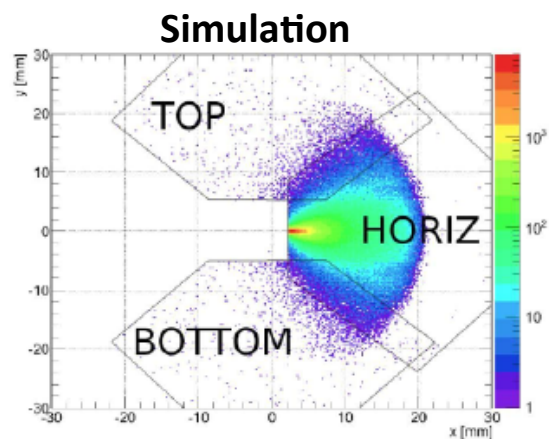
- ▷ Micro-strip silicon detectors with edgeless technology (inactive edge $\sim 50 \mu\text{m}$)
- ▷ 512 strips at $\pm 45^\circ$
- ▷ Pitch: $66 \mu\text{m}$
- ▷ Digital readout provided by VFAT2 chips
- ▷ Lifetime up to an integrated flux of $5 \times 10^{14} \text{ p/cm}^2$
→ too low for PPS requirements, detector pushed to its limit
- ▷ Hit/track reconstruction using consolidated TOTEM algorithms (software fully integrated in CMS official software)
- ▷ No multi-track capability
- ▷ Track resolution $\sim 12 \mu\text{m}$



Planar technology + CTS (Current Terminating Structure)



[*] TOTEM Coll., JINST 3 (2008) S08007

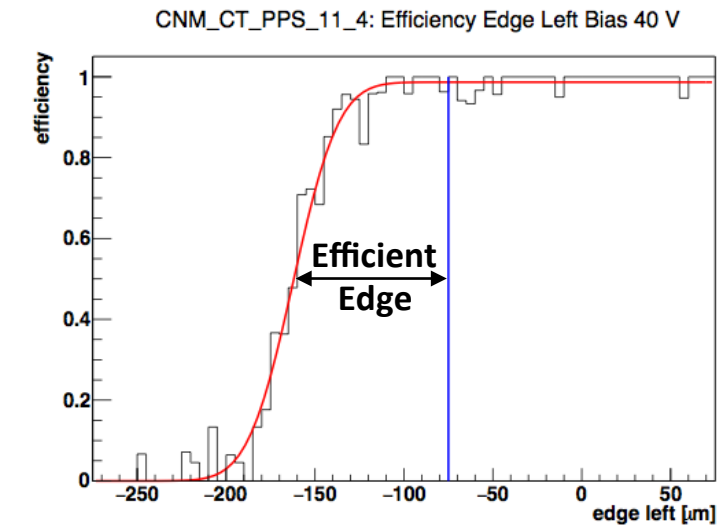
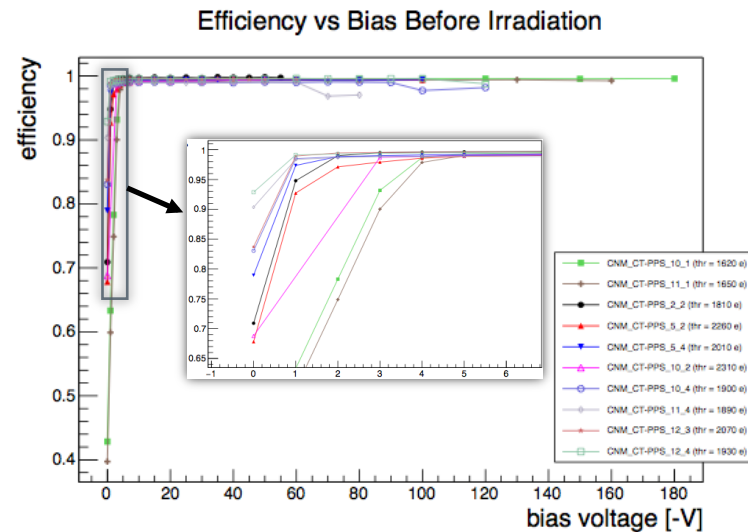


Tracking detector - Silicon 3D pixels



6 planes per pot of 3D silicon pixel detectors

- ▷ 3D sensor in double-sided not fully passing-through technology
- ▷ Intrinsic radiation hardness → to withstand overall integrated flux of 5×10^{15} p/cm²
- ▷ 200 μm slim edge → to approach the beam as much as possible
- ▷ Pixel dimensions: $100 \times 150 \mu\text{m}^2$ → very high granularity
- ▷ Resolution $< 30 \mu\text{m}$
- ▷ Planes tilted by 18.4° to optimize efficiency and resolution
- ▷ Front-end chip: latest version of PSI46dig^[*], same as for the CMS Pixel detector
- ▷ Operation at about -20°C and in vacuum ($p < 20$ mbar)
- ▷ Very good performance, bad pixels (efficiency $< 90\%$) less than 0.05% of all channels



[*] F. Meier, PSI46dig pixel chip External Specification Manual (2013)

Silicon 3D pixel sensors

3D sensor technology chosen because of its high radiation hardness and possibility to implement slim edges

Sensors produced by CNM with double-sided process and non-passing-through columns

Pixel size: 150x100

Sensor thickness: 230

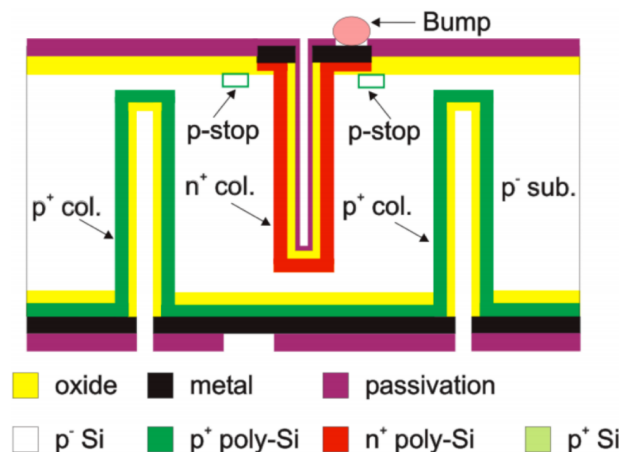
Column depth: 200

Column diameter: 10

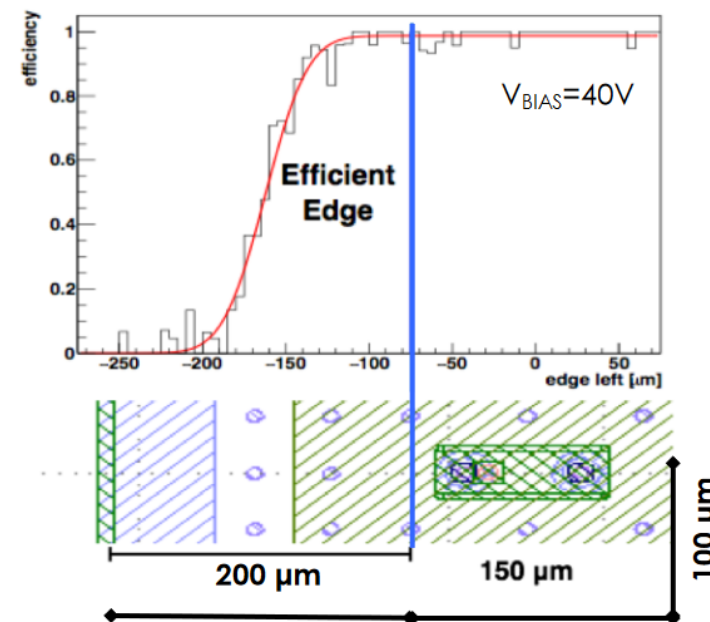
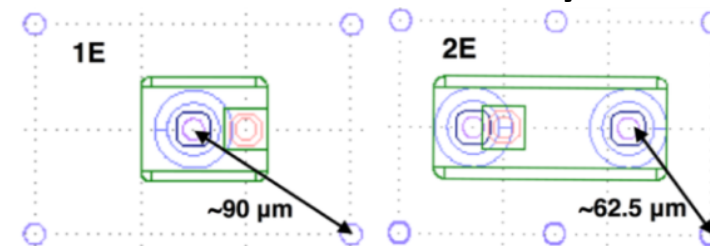
Depletion voltage: 5-10 V

3D sensors bump-bonded to the PSI46dig ROC were extensively tested in laboratory and with beam, at FNAL [*]

- ✓ 200 slim edge made of triple p-type column fence.
Reduced to 50 by increasing the bias voltage (for 2E type)
- ✓ **Spatial resolution for 2E(1E) electrode configuration**, with sensors tilted by 20°: **22 (25) μm**



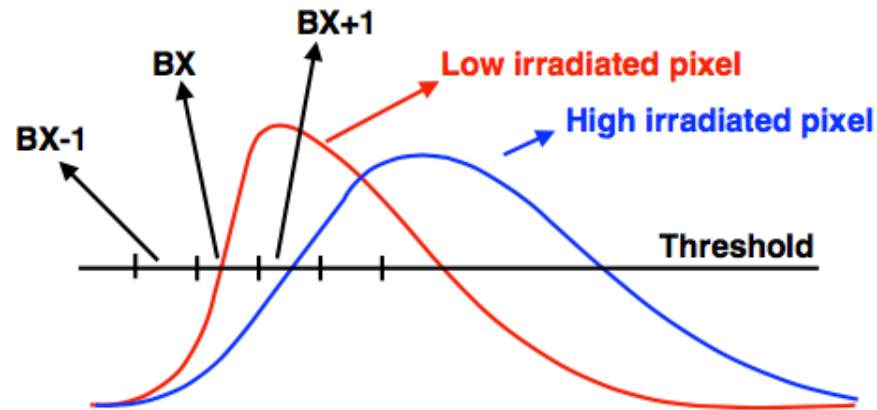
1E and 2E electrode layout



[*] F. Ravera, *The CT-PPS tracking system with 3D pixel detectors*, Pixel 2016 Workshop

Radiation damage of the 3D pixels readout chip

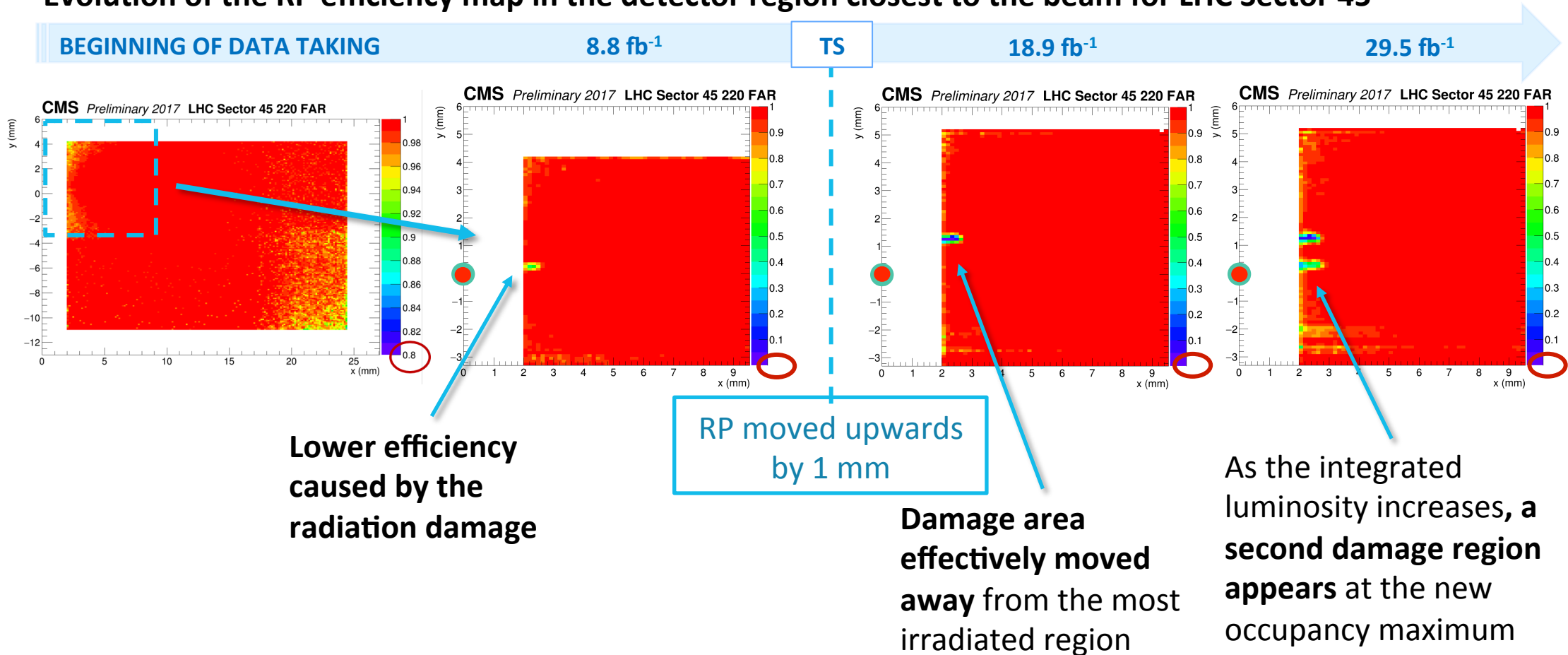
- The ROC used in CT-PPS is the same as that in layers 2-3-4 of the CMS central pixel detector
- The chip was not optimised for non-uniform irradiation
- After several irradiation tests, it has been understood that a non-uniform irradiation causes a difference between the analog current supplied to the most and the least irradiated pixels.
- The net result is that the amplified signal is slowed down and is associated to the following 25 ns clock window (BX):



- The irradiation studies showed that the effect appears after an irradiation compatible with a collected integrated luminosity $\sim 8 \text{ fb}^{-1}$. To mitigate the impact on the data quality, the tracking stations have been lifted during Technical Stops to shift the occupancy maximum away from the damaged region

3D pixel detector efficiency (2017)

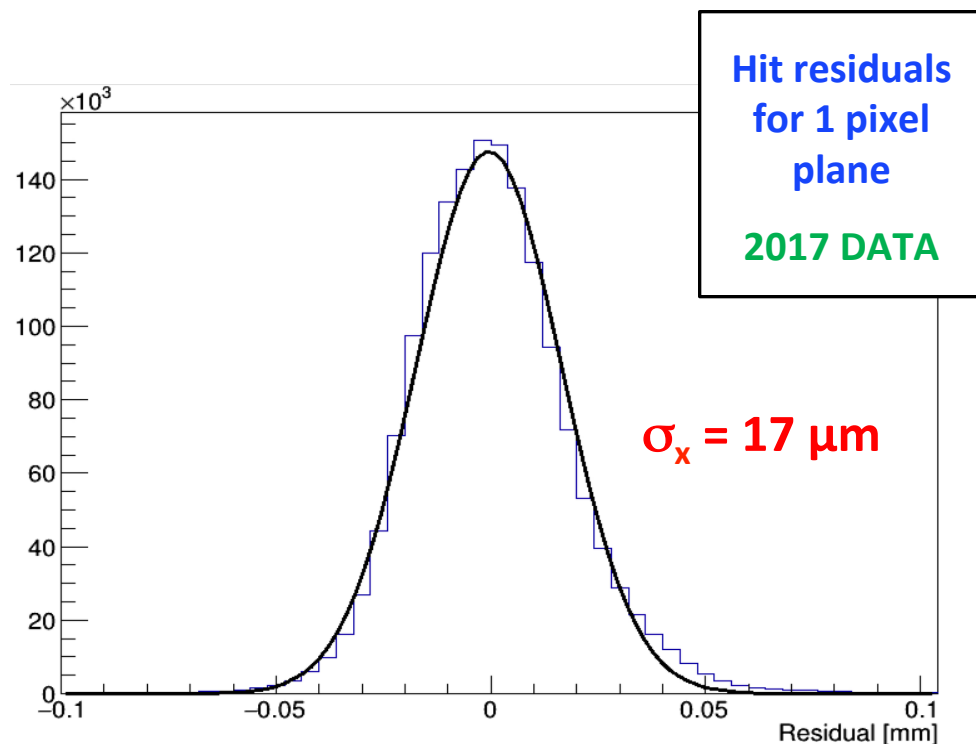
Evolution of the RP efficiency map in the detector region closest to the beam for LHC Sector 45



Detectors in LHC Sector 56 suffered smaller radiation damage (barely visible in the maps) because of the different irradiation profile

3D pixel tracker performance: hit resolution

Hit residuals for single planes are evaluated with respect to the local track reconstructed in the Pixel RP



- Residuals are consistent with those obtained at the beam tests
- Similar results in 2018

- ✓ The pixel tracker works as expected
- ✓ Track resolution under final evaluation ($\sim 20 \mu\text{m}$)

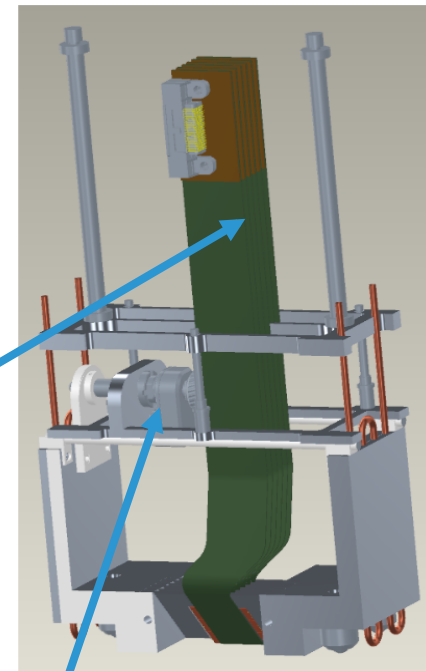
Tracking detectors for LHC-Run3

PPS will operate as a full CMS subsystem in LHC-Run3 (2022 - 2024)

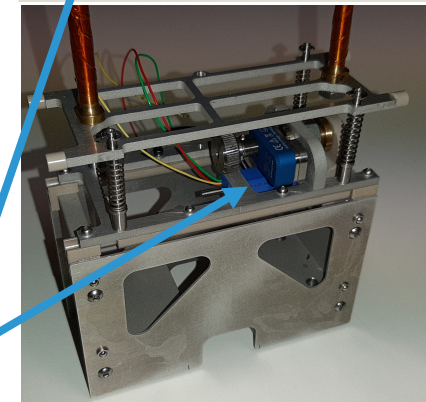
TRACKER SYSTEM in LHC-Run3

- 2 Roman Pots per side, at 210 m and 220 m from CMS-IP; 6 detector planes per RP (same as 2018)
- New **3D silicon pixel sensors** produced by FBK
 - ✓ Singl- side technology
 - ✓ 2x2 sensor geometry
 - ✓ 150 μm thick
 - ✓ 2E electrode configuration
- ROC: **PROC600** (same as layer 1 of the CMS pixel detector)
- **New flex circuit design** (different 'look' but very similar design)
- **New detector package with internal movement system**, to better distribute the radiation damage
 - 12 positions spaced by 500 μm , possibility of handling more than 50 fb^{-1} with minimal efficiency loss

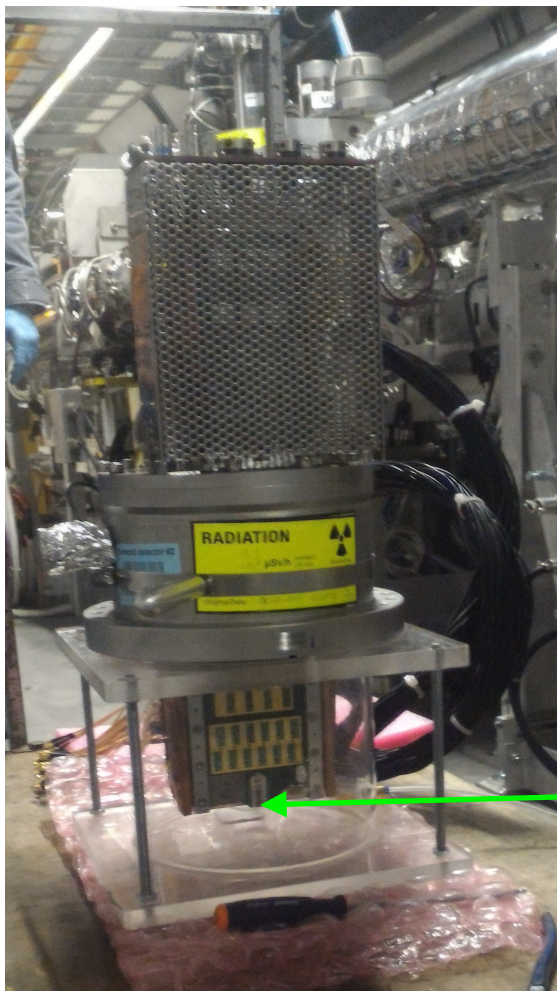
New flex circuit



Piezoelectric motor

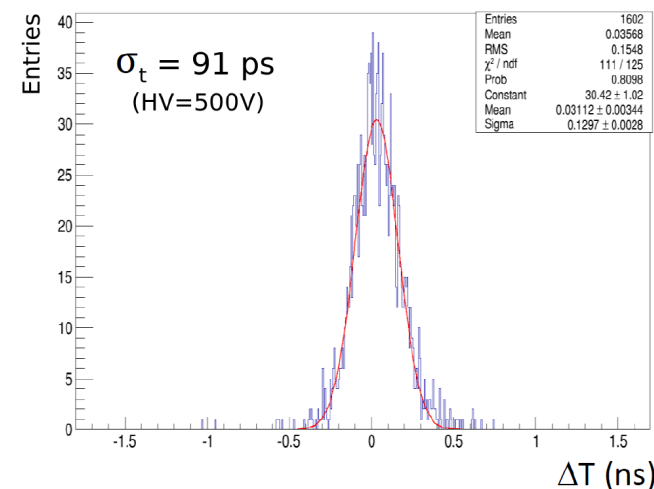
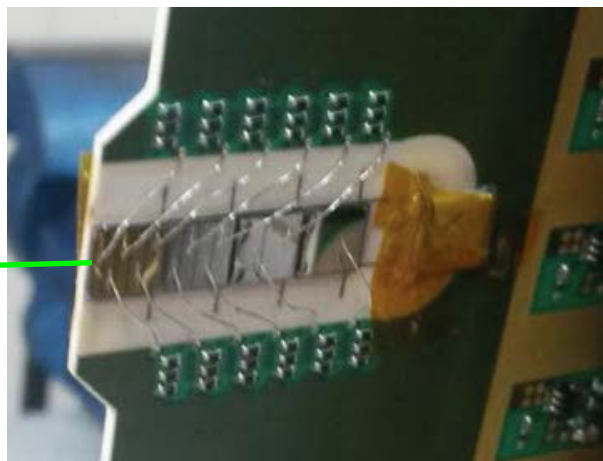


Timing detector - Diamonds



scCVD Diamond planes

- ▷ Four 4x4mm² diamond sensors per plane, 500μm thick, with different pad patterns
- ▷ Intrinsic radiation hardness → to withstand overall integrated flux of 5x10¹⁵ p/cm²
- ▷ Allow for high granularity (wrt to, e.g., quartz)
- ▷ Time resolution ~ 80 ps per plane
- ▷ Amplification with TOTEM hybrid^[1]
- ▷ Readout with NINO chip^[2] + HPTDC^[3]



Time resolution for the detector prototype as measured in a test run in 2015

[1] TOTEM Coll., JINST 12 (2017) P03007

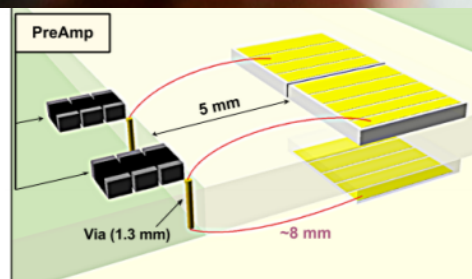
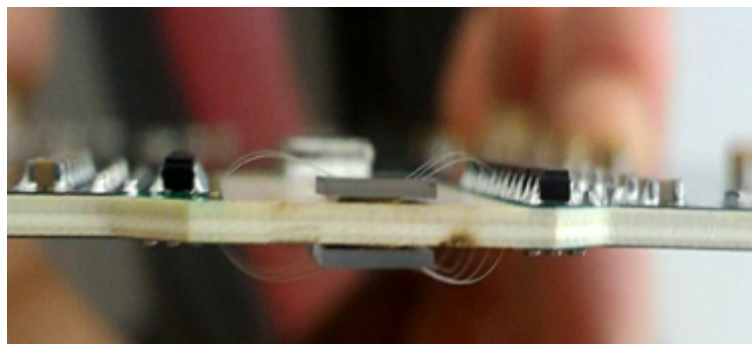
[2] F. Anghinolfi et al., NIM A 533 (204) 183

[3] M. Mota and J. Christiansen, IEEE JSSC 34 (1999) 1360

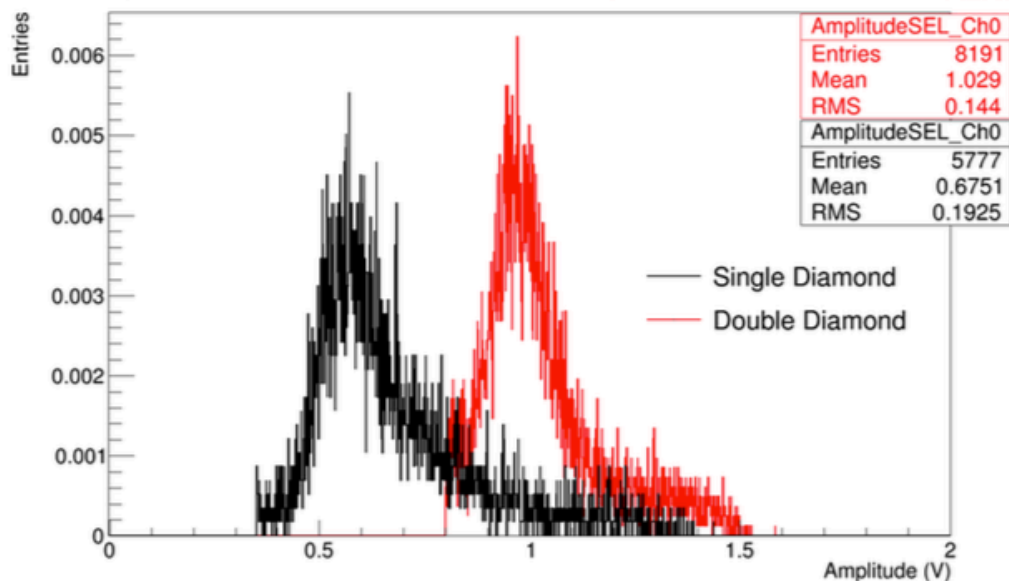
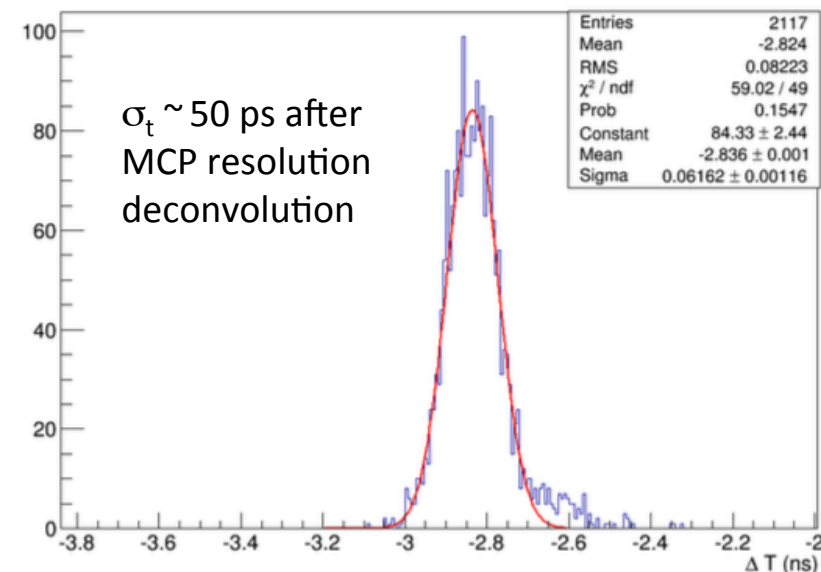
Timing detector - Double diamonds

Double-diamond planes

For improving the timing resolution of the diamond detector, two scCVD sensors (installed back to back) have been connected to the same amplifier channel, thus resulting in a timing resolution of 50 ps per plane as measured in a beam test^[*].



Time difference distribution between double diamond detector and MCP



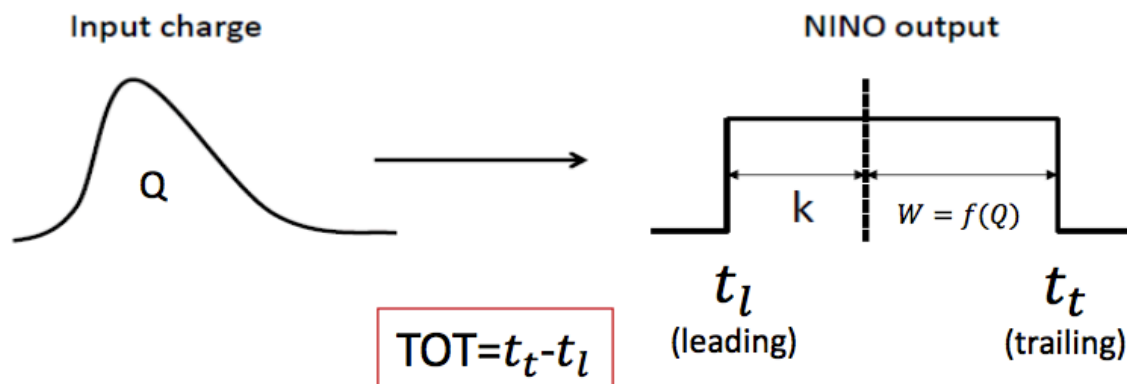
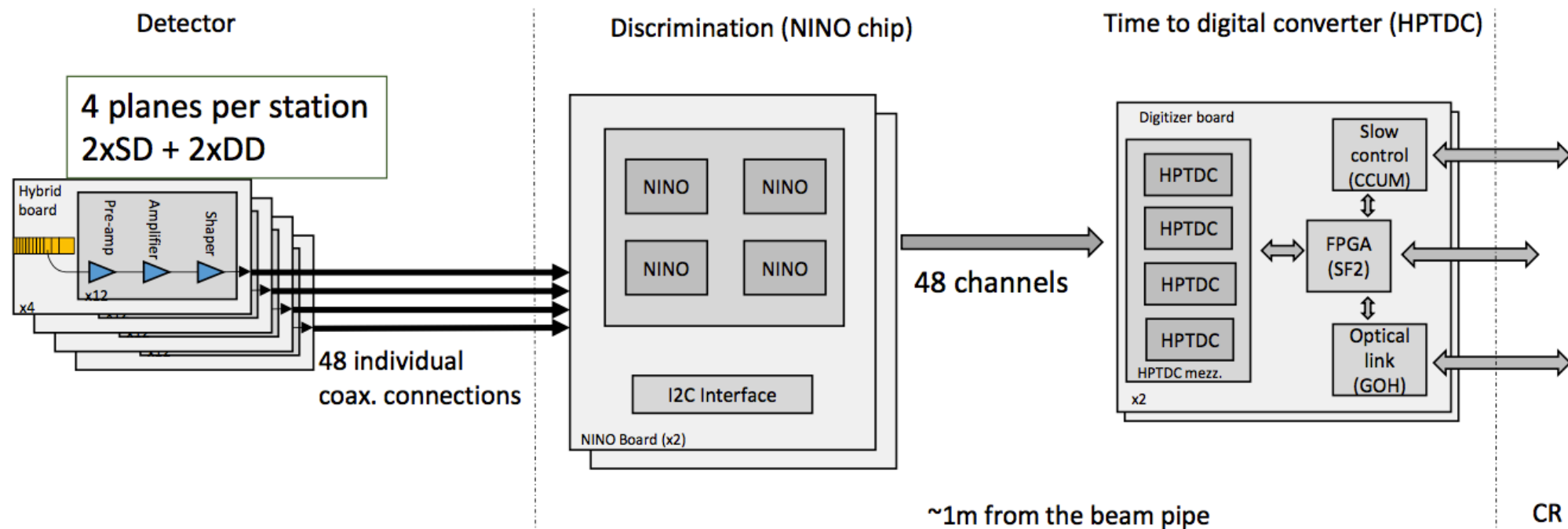
Signal from corresponding pads is connected to the same amplification channel:

- Higher signal amplitude
- Same noise (pre-amp dominated) and rise time (defined by shaper)
- Higher sensor capacitance
- Need a very precise alignment

Better time resolution w.r.t SD (factor ~ 1.7)

[*] M. Berretti et al., JINST 12 (2017) P03026

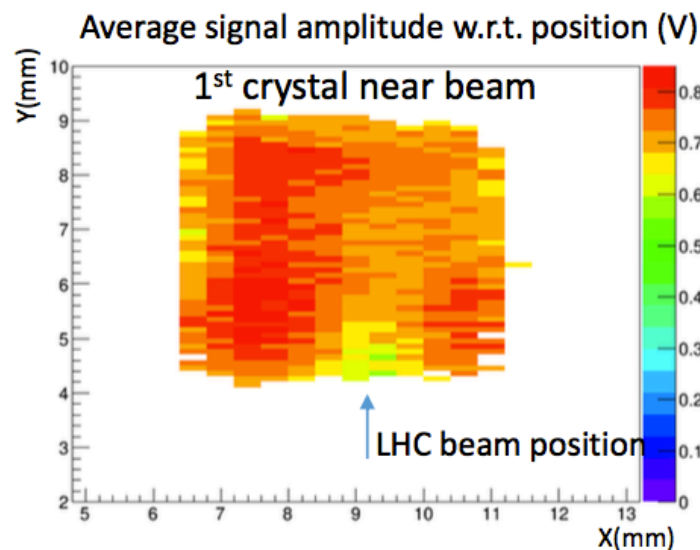
Timing detector layout in LHC-Run2



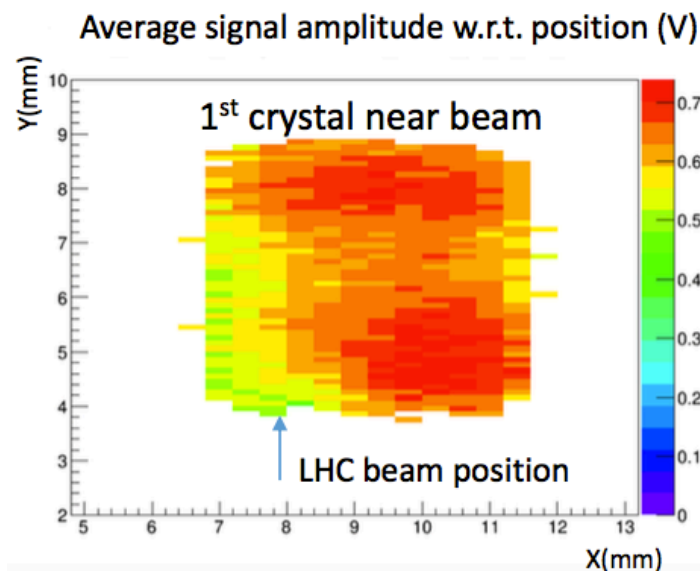
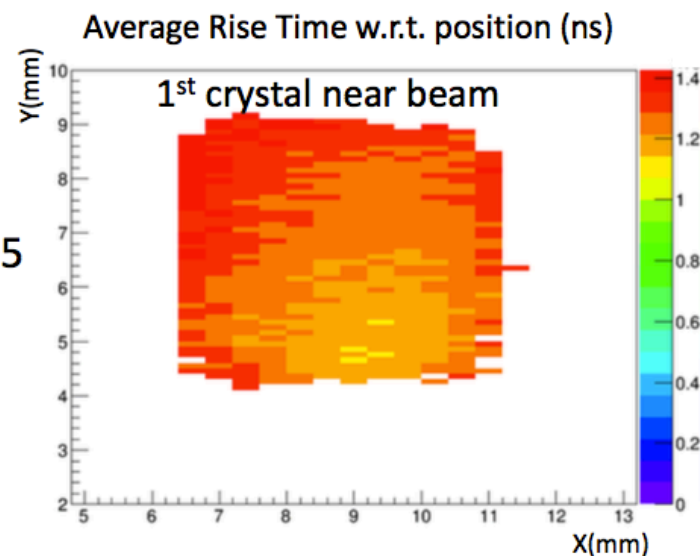
In Run 2 discrimination stage degraded timing performance by 30% (after time walk correction).

Optimization ongoing for Run 3

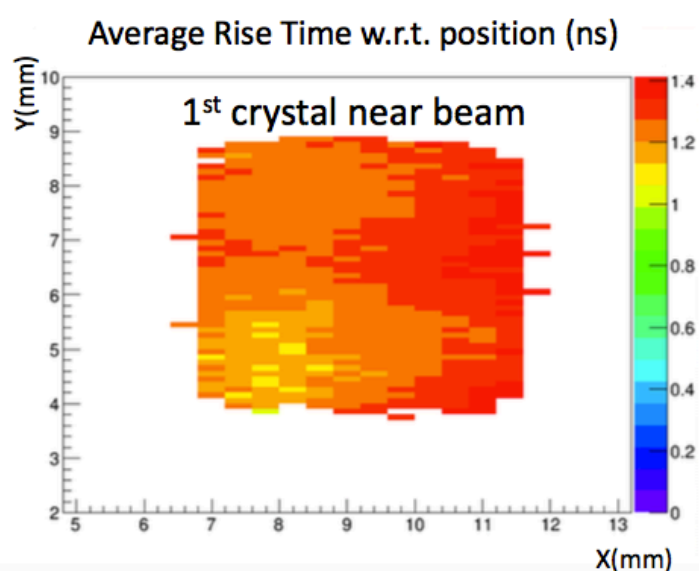
Timing detector: localized damage in DD



Sector 45



Sector 56



Sensors used in 2018 have been tested in DESY test beam facility with 4.8 GeV electrons. Tracker available to perform position dependent measurements.

Test beam settings:

- nominal LV
- HV @ 500V

Reduction of signal observed in the area with highest irradiation, partially compensated by faster rise time.

The measurements leading to these results have been performed at the Test Beam Facility at DESY Hamburg (Germany), a member of the Helmholtz Association (HGF)

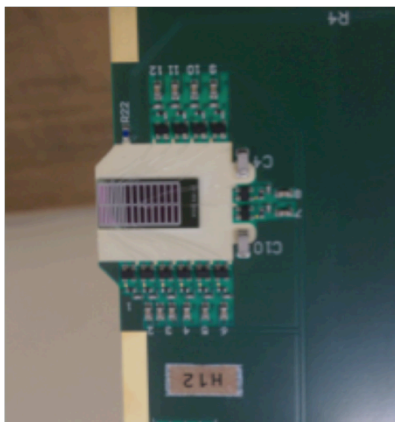
Timing detectors for LHC-Run3

Important upgrade program ongoing for the timing system:

- New hybrid boards -> increase in amplification stability and HV isolation, further optimization of performance
- New discriminator board (still based on NINO chip) -> reduce timing degradation in digitization phase
- Amplification LVs will be remotely controlled
- Sensor readout with SAMPIC chip (fast sampler @ 7.8 Gsa/s) will be available for commissioning phase and sensor monitoring (cannot sustain hit rate at nominal luminosity). Successfully used as CMS-TOTEM timing sensor readout for a special run in 2018 (lower hit rate, Ultra Fast Silicon Detectors as sensor) [PoS TWEPP2018 (2019) 137] :
 - ▷ Improvement of calibration quality
 - ▷ Fast feedback from settings modification
 - ▷ Monitor of sensor performance (disentangled from digitization stages)
 - ▷ Parallel readout -> No impact on regular data acquisition
- An additional timing station will be built and installed in each sector.
Each station will be equipped with 4 DD planes → 8 DD planes in each sector.

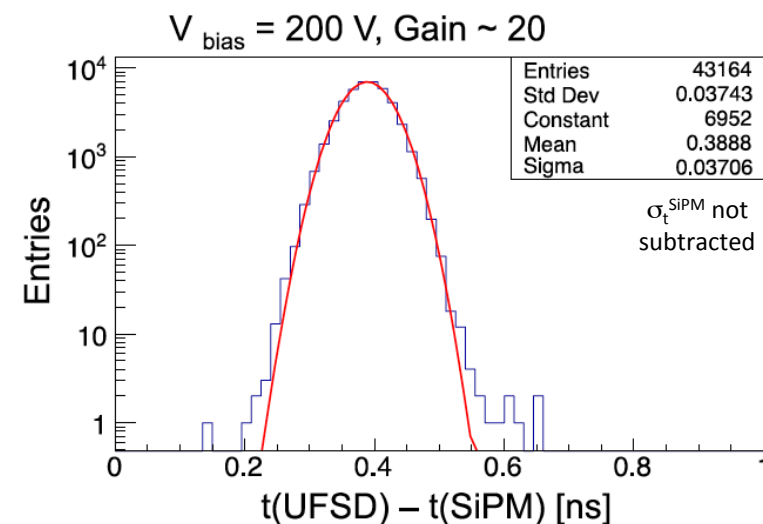
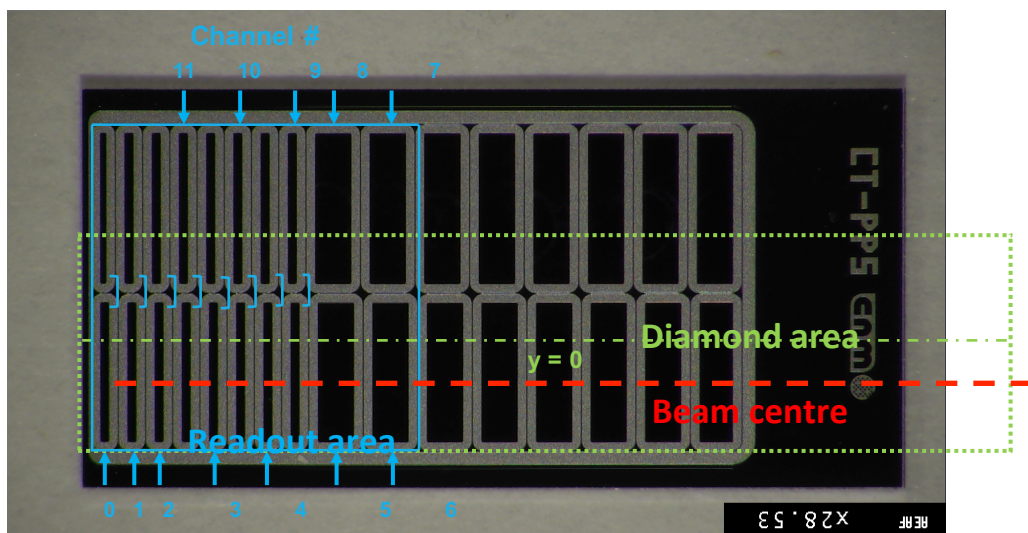
Ultimate resolution goal (< 30 ps) within reach

Timing detector - UFSD



UFSD planes - First installation in HEP, 1 plane in 2017

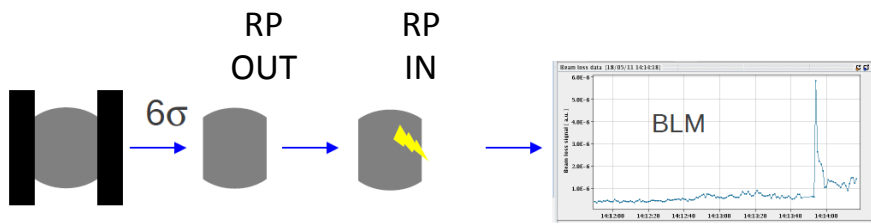
- ▷ Eight $0.5 \times 6 \text{ mm}^2$ pads, four $1 \times 3 \text{ mm}^2$ pads
- ▷ Radiation hardness still an issue \rightarrow in RP environment ($T > 30^\circ\text{C}$) lifetime $\lesssim 10^{15} \text{ p/cm}^2$
- ▷ Allow for high granularity (wrt to, e.g., quartz)
- ▷ Time resolution $\sim 35 \text{ ps}$ per plane^[*]
- ▷ Amplification with modified TOTEM hybrid^[2]
- ▷ Readout with NINO chip^[3] + HPTDC^[4]



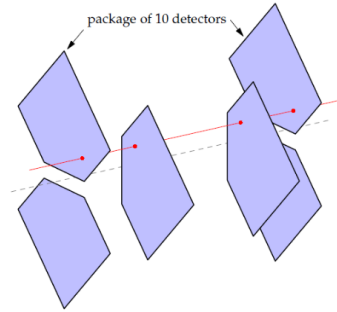
[*] N. Cartiglia et al., NIM A 850 (2017) 83

Alignment & optics

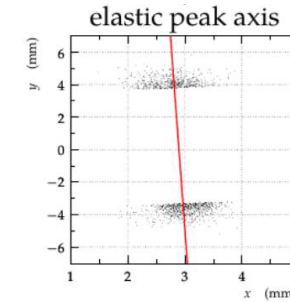
To validate each optics configuration, a low intensity run is required where also the TOTEM vertical RP approach the beam, allowing to align the RPs among themselves (2.) and wrt the beam (3.)



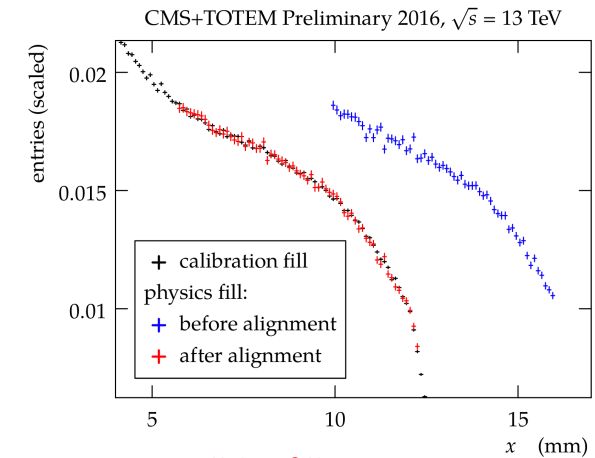
1. Alignment wrt the collimators



2. Relative RP alignment



3. Global alignment wrt the beam using elastic scattering



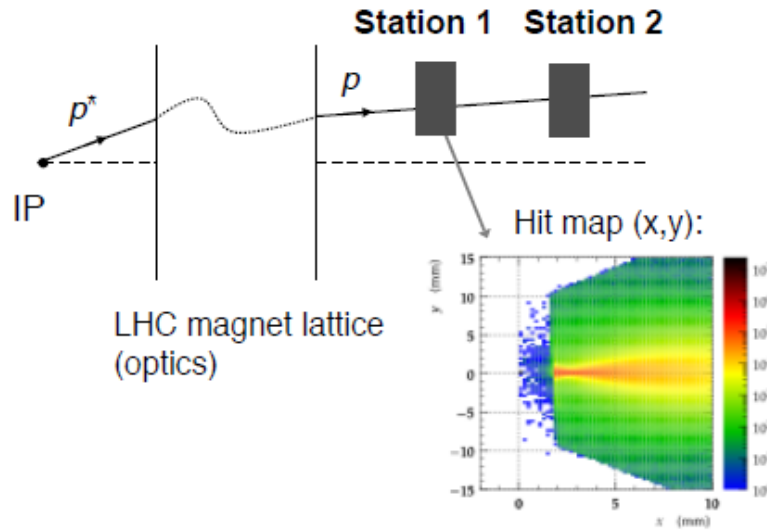
4. Fill-by-fill comparison of hit X distribution

For each physics run, the RP position can be determined by comparing the measured shape of the X distribution with the one obtained in the alignment run (4.)

A detailed knowledge of the LHC optics is essential to correctly reconstruct the proton fractional momentum loss ξ LHC magnetic model is adjusted to match measurements from RP and beam position monitors

[CERN-TOTEM-NOTE-2017-002]

Proton reconstruction

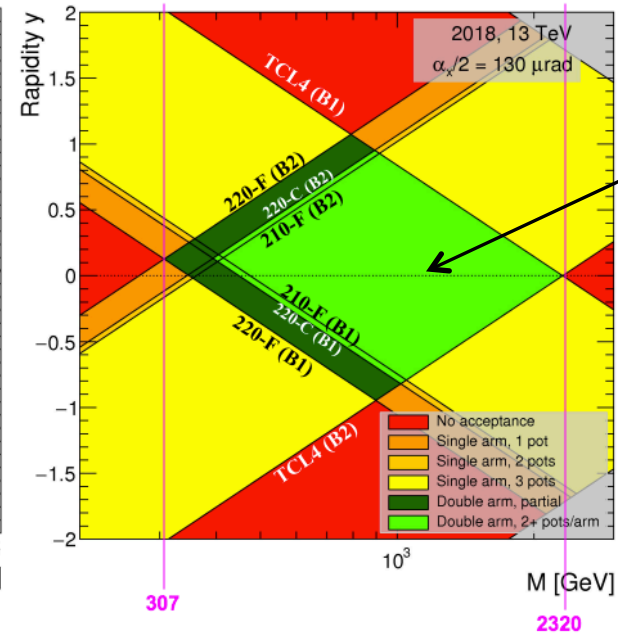
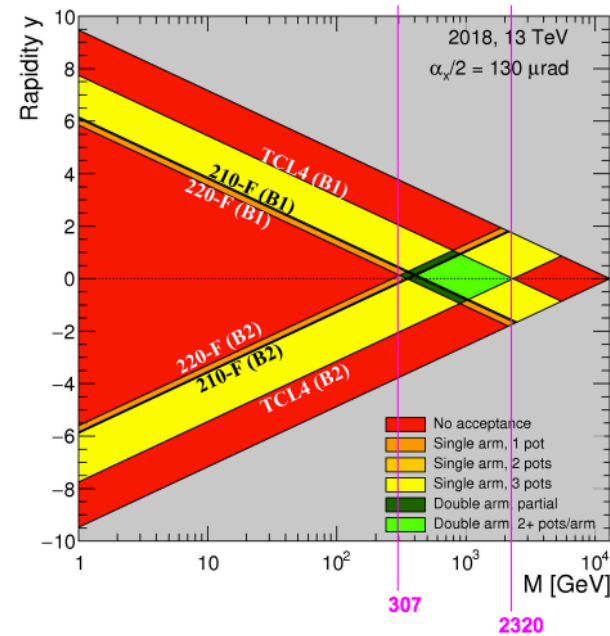


Knowledge of the beam optics allows the proton fractional momentum loss ξ to be computed, from which the invariant mass and the rapidity of the centrally produced state X are determined

$$\xi = 1 - \frac{|p_f|}{|p_i|} \quad M_X = \sqrt{s \xi_1 \xi_2} \quad y_x = \frac{1}{2} \log\left(\frac{\xi_1}{\xi_2}\right)$$

Double arm mass acceptance in the ~400-2000 GeV range:

- lower limit mainly due to the minimum distance from the beam (may vary depending on beam conditions, e.g. crossing angle)
- upper limit due to collimators



Proton transport model

- The propagation of the proton from the IP to the RPs is approximately modeled with this linear formula:

$$\mathbf{d}(s) = T(s) \cdot \mathbf{d}^*$$

where $\mathbf{d} = \left(x, \theta_x, y, \theta_y, \frac{\Delta p}{p} \right)^T$, the * symbol refers to quantities at the IP,

$$T = \begin{pmatrix} v_x & L_x & m_{13} & m_{14} & D_x \\ \frac{dv_x}{ds} & \frac{dL_x}{ds} & m_{23} & m_{24} & \frac{dD_x}{ds} \\ m_{31} & m_{32} & v_y & L_y & D_y \\ m_{41} & m_{42} & \frac{dv_y}{ds} & \frac{dL_y}{ds} & \frac{dD_y}{ds} \\ 0 & 0 & 0 & 0 & 1 \end{pmatrix}, \begin{cases} v_{x,y} = \sqrt{\beta_{x,y}/\beta^*} \cos(\Delta\mu_{x,y}) \\ L_{x,y} = \sqrt{\beta_{x,y} \cdot \beta^*} \sin(\Delta\mu_{x,y}) \end{cases}$$

β is the betatron amplitude and $\Delta\mu_{x,y}$ is the relative phase advance ($\Delta\mu_{x,y} = \int_{IP}^{RP} \frac{ds}{\beta_{x,y}}$)

The leading terms are:

- $x \approx D_x(\xi) \cdot \xi$
- $y \approx L_y(\xi) \cdot \theta_y^*$

2018 RP acceptance

